OXFORD CDE

Journal of Computational Design and Engineering, 2022, 9(2), 330–342

https://doi.org/10.1093/jcde/qwac002
Journal homepage: www.jcde.org

RESEARCH ARTICLE

Benchmarking anthropomorphic hands through grasping simulations

Immaculada Llop-Harillo *, José L. Iserte and Antonio Pérez-González

Departamento de Ingeniería Mecánica y Construcción, Universitat Jaume I (UJI), Castellón 12071, Spain

*Corresponding author. E-mail: illop@uji.es http://orcid.org/0000-0002-9378-1947

Abstract

In recent decades, the design of anthropomorphic hands has been developed greatly improving both cosmesis and functionality. Experimentation, simulation, and combined approaches have been used in the literature to assess the effect of design alternatives (DAs) on the final performance of artificial hands. However, establishing standard benchmarks for grasping and manipulation is a need recognized among the robotics community. Experimental approaches are costly, time consuming, and inconvenient in early design stages. Alternatively, computer simulation with the adaptation of metrics based on experimental benchmarks for anthropomorphic hands could be useful to evaluate and rank DAs. The aim of this study is to compare the anthropomorphism of the grasps performed with 28 DAs of the IMMA hand, developed by the authors, using either (i) the brute-force approach and grasp quality metrics proposed in previous works or (ii) a new simulation benchmark approach. The new methodology involves the generation of efficient grasp hypotheses and the definition of a new metric to assess stability and human likeness for the most frequently used grasp types in activities of daily living, pulp pinch and cylindrical grip, adapting the experimental Anthropomorphic Hand Assessment Protocol to the simulation environment. This new simulation benchmark, in contrast to the other approach, resulted in anthropomorphic and more realistic grasps for the expected use of the objects. Despite the inherent limitations of a simulation analysis, the benchmark proposed provides interesting results for selecting optimal DAs in order to perform stable and anthropomorphic grasps.

Keywords: artificial hand anthropomorphism; benchmarking; grasping simulation; prosthetic hand design

List of Abbreviations

ADL:	Activities of Daily Living.
AHAP:	Anthropomorphic Hand Assessment Protocol.
CG:	Cylindrical Grip.
CMC:	Carpometacarpal.
DAs:	Design Alternatives.
DoFs:	Degrees of Freedom.
GAS:	Grasping Ability Score.
GHs:	Grasp Hypotheses.
GQM:	Grasp Quality Metrics.
GTs:	Grasp Types.
MCP:	Metacarpophalangeal.
PP:	Pulp Pinch.
S_{GAS}:	Simulated Grasping Ability Score.
YCB:	Yale-CMU-Berkeley.

Nomenclature

P :	Approach reference point in the hand.
$\boldsymbol{n}$:	Approach direction vector in the hand.
$\boldsymbol{n}_{palmar}$:	Palmar normal vector in the phalanx.
$\boldsymbol{n}_{main}$:	Vector that defines the thumb main axis direction.

Received: 6 September 2021; **Revised:** 16 December 2021; **Accepted:** 20 December 2021

$\boldsymbol{n}_{\text{contact}}$: Normal contact vector.
d : Distance between the points in the cartesian grid of the bounding box.
α : Apex angle of the cone containing the approach rays.
N_α : Number of approach rays distributed inside the cone with angle α.
δ : Standoff distance at which the palm of the hand stands still and the grip begins.
N_δ : Number of standoff distances.
θ : Angle to rotate the hand (roll) about the approach ray.
θ_{i} : Initial roll angle with respect to vector $\boldsymbol{n}$.
θ_{f} : Final roll angle with respect to vector $\boldsymbol{n}$.
N_θ : Number of rolls uniformly distributed between θ_{i} and θ_{f}.
N_{GH} : Total number of grasp hypotheses tested per object.
FC : Number of grasps that accomplish the force-closure condition.
C : Number of correct grasps according to the grasp-type correctness criteria among those satisfying the force-closure condition.
NC : Number of not correct grasps according to the grasp-type correctness criteria among those satisfying the force-closure condition.

1. Introduction

Artificial hands are used in both robotics and prosthetics to provide grasping abilities to either robots or people with upper-limb limitations. Anthropomorphic hands are becoming popular, especially in the last decades, driven by the need to improve cosmesis but also as a means to improve the functionality. However the unmatched functionality and aesthetics of the human hand are still far to be achieved with current technology (Jang *et al.*, 2011; Belter *et al.*, 2013). Among the different factors that limit the functionality of current artificial hands for grasping or manipulating objects, one of the first to be considered in design is the kinematic chain configuration. Specifically, the number of segments per finger and the orientation of the thumb and finger joints affect the achievable grasping postures and thus the final functionality.

Experimentation, simulation, and combined approaches have been used in the past to analyse the effect of the artificial hand design on its final performance. Experimental approaches allow assessing the grasping ability of artificial hands with realistic information about the final performance. Establishing standard benchmarks for grasping and manipulation is a need recognized among the robotics community (Calli *et al.*, 2015; Falco *et al.*, 2015). Quispe *et al.* (Huamán Quispe *et al.*, 2018) proposed a general taxonomy for benchmarking manipulation tasks and described recommendations about how to define useful testing protocols. The authors have recently proposed a protocol (Llop-Harillo *et al.*, 2019) to quantify functionality and human likeness of anthropomorphic hands while grasping objects of daily living. However, experimental approaches are costly and time consuming and require the use of physical prototypes, which is unsuitable in early design stages. Alternatively, computer simulation can be useful to evaluate and rank design alternatives (DAs). Some studies (Feix *et al.*, 2013; Liarokapis *et al.*, 2013) proposed anthropomorphism indexes based on the comparison of the workspace of the artificial hand and that of the human hand. However, a limitation of this approach is the fact that the indexes are based only on the comparison of the reachable positions for the hand but do not consider the position of all the contact points of the hand with actual objects. Consequently, the final grasp stability obtained with different hand designs cannot be evaluated.

In robotics, the problems of grasp simulation and grasp planning have been extensively analysed (Sahbani *et al.*, 2012). Grasp planning involves determining a hand configuration and a set of feasible contact points between the hand and the object to be grasped in order to reach force closure, equilibrium or stability, among other possible objectives. In order to decide the best grasping strategy, quantification of the grasp quality of a given object–hand–posture set is needed and different grasp quality metrics (GQMs) have been proposed in the literature. Roa and Suarez (Roa & Suárez, 2014) made an extensive survey of most of these metrics. Rubert and Morales (Rubert & Morales, 2016) compared the use of 10 selected GQMs with the use of the anthropomorphism index proposed by Feix *et al.* (Feix *et al.*, 2013) in order to evaluate the performance of different anthropomorphic hands, concluding that both approaches are not equivalent. In that work, they also noted a low correlation among the 10 GQMs when evaluating the same set of grasps. A low correlation among GQM was also found in a different study by the same authors with other hands and objects (Rubert *et al.*, 2017). The use of combined metrics has been suggested as a method to find a more robust estimator of the grasp quality (Roa & Suárez, 2014), although an optimal solution has not been found. Despite these limitations, the use of GQM for evaluating the ability of a robotic or prosthetic hand design for achieving successful grasps can be considered as an alternative to costly experimentation and prototyping in the initial design stages.

A rather limited number of simulation tools have been proposed in the past in the robotics community for grasping simulation. GraspIt (Miller & Allen, 2004) is one of the pioneering tools made available to researchers (http://graspit-simulator.github.io/), and included the models for some popular robot hands. OpenRAVE (Diankov, 2010) is a general environment for testing, developing, and deploying motion planning algorithms in real-world robotics applications. With respect to GraspIt, OpenRAVE has the advantage of having a modular design, simplifying extension and further development. The open architecture and modular design allow a simple integration of simulation, visualization, planning, scripting, and control of robot systems. OpenGrasp (http://opengrasp.sourceforge.net/; León *et al.*, 2010) was developed as a toolkit to simulate grasping within the framework of OpenRAVE (http://openrave.org/). OpenGrasp completes OpenRAVE including improvements in the use of different physics simulation engines and also incorporates a robot editor based on the use of the COLLADA™ file format (https://www.khronos.org/collada/). A version of OpenGrasp, named OpenHand, including also a biomechanical model to simulate grasping with the human hand was later developed by León (León *et al.*, 2014) in collaboration with the authors' research group. This version is publicly available at https://sites.google.com/a/uji.es/devalhand/openhand-simulator. OpenHand presents a graphical user interface for automatic generation of grasp hypotheses (GHs) and implements the computation of several GQMs to evaluate the final grasps.

In OpenRAVE, the grasping problem can be faced with the brute-force paradigm by means of its Grasping Module (Rubert *et al.*, 2017). For generating the GHs for a given object and hand, a cartesian grid of points is generated in the surface of a bounding box around the object and projected over its surface. From these points on the surface, a series of approach rays are generated, defining different grasp approaches for the hand. This generation of GHs is dependent on several parameters such as: the

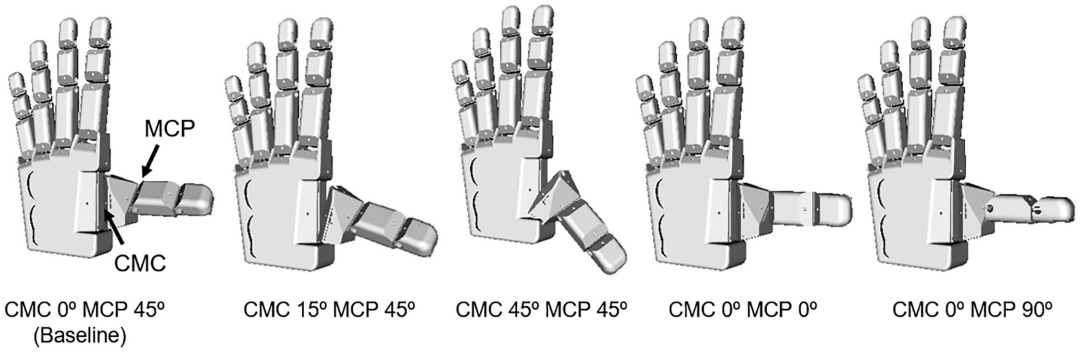

Figure 1: Some of the 28 IMMA hand DAs. Thumb CMC and MCP joint orientation indicated.

distance between the points in the cartesian grid of the bounding box; the angle between the approach rays and the normal to the object surface; the standoff distance at which the palm of the hand stands still and the grip begins; and the angle to rotate the hand about the approach ray. For a given set of values for these parameters, a set of GHs corresponding to initial positions and orientations of the hand with respect to the object is generated.

The brute-force approach has the advantage of being general and applicable to any hand or object, being useful for facing the grasp planning in a robotic environment (Morales *et al.*, 2004; Pinto & Gupta, 2016; Levine *et al.*, 2018). However, the use of this method presents some major drawbacks. First, it requires a long time to compute a reasonable sample. Second, some of the GHs generated are redundant for objects presenting some kind of symmetry. Third, and particularly relevant in applications such as prosthetics, service robotics, and human–robot cooperation, most of the final grasps obtained are not realistic for activities of daily living (ADLs). Moreover, for simulating the grasping performance of a prosthetic hand, it seems practical to limit the GHs exploiting the human experience for grasping the objects, because in the actual use of the prosthesis the human brain would guide the arm motion to an adequate position and orientation of the wrist for the intended grasp. The use of human oriented approaches could solve some of these limitations. The selection of GHs inspired by the human hand was used in León *et al.* (León *et al.*, 2013) to compare GQMs obtained with the Michelangelo hand and with the biomechanical model of the human hand included in OpenHand. The use of grasp planning based on human demonstration has also allowed to reduce both the feasible workspace and the search space in robotic applications (Lin & Sun, 2015). Finally, the use of grasping simulation for prosthetic design requires a better definition of the outcome parameters. The adaptation of metrics based on experimental benchmarks for anthropomorphic hands could be an alternative.

The final aim of this study is to present a new approach for evaluating anthropomorphic hands based on grasping simulation and assessment within the framework of the OpenRAVE simulation tool. This methodology involves the use of human knowledge for the generation of efficient GHs and the definition of a new metric to assess human likeness of the achievable grasps with the artificial hand. To this end, we propose to adapt the Anthropomorphic Hand Assessment Protocol to a simulation environment (AHAP; Llop-Harillo *et al.*, 2019). The AHAP is an experimental benchmark for grasping ability that considers the most common grasp types (GTs) during ADL using everyday objects. To exemplify the methodology, a comparison of 28 different DAs for the IMMA hand, an anthropomorphic prosthetic hand developed by the authors (Llop-Harillo & Pérez-González, 2017a), was performed. The two most frequently used GTs (pulp pinch and cylindrical grip) of those included in the AHAP were covered in this study, although the methodology can be easily extended including the eight main GTs included in the AHAP (pulp pinch, lateral pinch, diagonal volar grip, cylindrical grip, extension grip, tripod pinch, spherical grip, and hook grip) (Llop-Harillo *et al.*, 2019). The results obtained using this new simulation benchmark were compared with the results obtained using the brute-force approach and the GQM proposed in previous works and included in OpenHand (León *et al.*, 2012, 2014; Rubert & Morales, 2016; Rubert *et al.*, 2017). This comparison has the aim of analysing whether the grasps generated with the brute-force approach that show good GQM correspond to realistic grasps in a human environment.

2. Methods

2.1. IMMA hand DAs

The IMMA hand is a tendon-driven prosthetic hand prototype designed by the authors (Llop-Harillo & Pérez-González, 2017a). The original design of this hand, considered as the baseline in this study, is publicly available at Llop-Harillo and Pérez-González (2017b). It includes six independently actuated degrees of freedom (DoFs): one for the flexion of each long finger, and two more in the thumb, for flexion and circumduction movements.

The combination of the orientation angles of the carpometacarpal (CMC) joint and the metacarpophalangeal (MCP) joint of the thumb allows the opposition of the thumb to orient its distal phalanx to the distal phalanges of the different long fingers. Therefore, with the aim of analysing the best combination of these orientation angles to perform the most relevant GTs in an anthropomorphic way, several DAs have been proposed modifying these joint orientations. Consequently, 28 DAs have been analysed: the combination of 4 different orientations for the thumb CMC joint (0º, 15º, 30º, and 45º with respect to the proximal–distal axis) and 7 for the thumb MCP joint (0º, 15º, 30º, 45º, 60º, 75º, and 90º with respect to the CMC axis). The thumb configuration of the baseline is CMC 0º and MCP 45º. Figure 1 shows some of these DAs, the baseline and those that illustrate the range of the joint angles.

2.2. Grasp types and objects

The AHAP (Llop-Harillo *et al.*, 2019) is an experimental benchmark based on 26 tasks involving grasping with the 8 most relevant human GTs during ADL and 2 nongrasping postures.

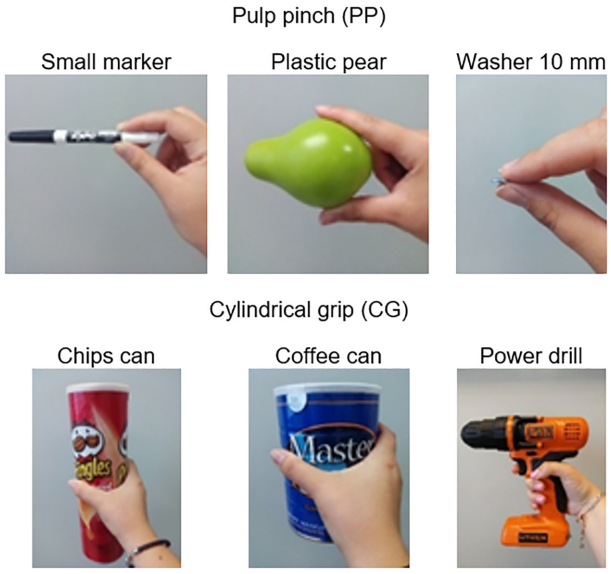

Figure 2: GTs and objects selected from the AHAP (Llop-Harillo *et al.*, 2019).

It quantifies the grasping ability of anthropomorphic artificial hands, including the human likeness and the grasp stability. The objects of the AHAP were selected from the Yale-CMU-Berkeley (YCB) set (Calli *et al.*, 2015) due to their public availability. The objects selected account for variations in size and shape. For the simulation analysis in this paper, the objects were modelled in SolidWorks by the authors (Pérez-González & Llop-Harillo, 2019). For the sake of simplicity, only the prehensile GTs with a frequency of use above 10% according to Vergara *et al.* (Vergara *et al.*, 2014) were used in this study: pulp pinch (PP) (38.3%) and cylindrical grip (CG) (12.3%). Figure 2 shows the six objects used in AHAP for the selected GTs and their approximate final position/orientation with respect to the artificial hand (Llop-Harillo *et al.*, 2019).

2.3. Grasp simulation: brute-force approach

The brute-force approach for grasping simulation is based on the Grasping Module from the Database Generators available in OpenRAVE (Rubert *et al.*, 2017). The GHs are generated based on the following parameters defined in OpenRAVE and shown in Fig. 3:

1. Distance between the points in the cartesian grid of the bounding box surrounding the object (d).
2. Apex angle of the cone containing the approach rays (α). The cone axis is defined by the normal to the reference point in the object.
3. Standoff distance at which the palm of the hand stands still and the grip begins (δ).
4. Angle to rotate the hand (roll) about the approach ray (θ).

In this study, the OpenRAVE parameters included in Table 1 were used to generate the GHs.

The same procedure was repeated for each hand and object (28 IMMA hand DAs and 6 objects):

1. The Grasping Module is used to generate a variety of GHs using the parameters presented in Table 1.
2. For each GH, only the most proximal hand joint of every finger closes with a common velocity until the contact with the

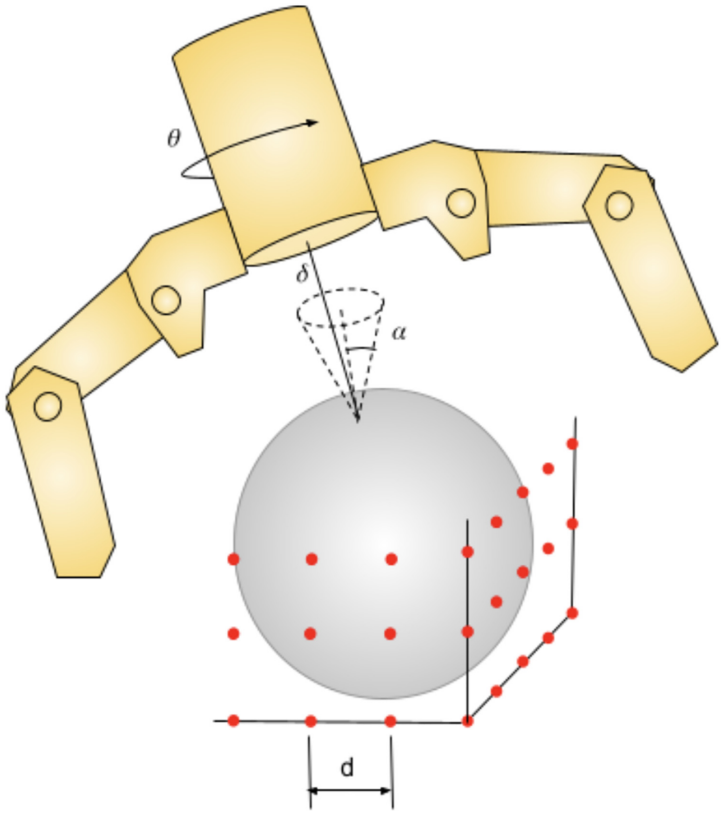

Figure 3: Parameters used in OpenRAVE for generating the GHs.

Table 1: Parameters: selected to generate GHs.

Parameter	Value(s)
d (mm)	20
α (rad)	0
δ (mm)	$\{0, 25\}$
θ (rad)	$\{0, \pi/2, \pi, 3\pi/2, 2\pi\}$

object is detected or the joint limit is reached. The process is repeated in the same way only for the joints located distally to the contacts. A final grasping posture is reached and the contact points are obtained.

3. The grasping posture is considered stable and defined as a *successful grasp* if the force-closure condition is accomplished. The grasp is in force closure when the hand can apply, through the set of contacts, arbitrary wrenches on the object. This means that contact forces impede any movement of the object (Nguyen, 1986). The simulation assumes that the hand can exert forces of any magnitude and the friction coefficient between all the objects and the hand is established in 0.4. Although the soft contact model is more accurate and has been used successfully in different simulation works (Ciocarlie *et al.*, 2005; Moisio *et al.*, 2012), the hard contact model with friction has been assumed. This model is sufficiently accurate for the purposes of the work and has the advantages of lower complexity and lower computational cost. In the simulation, the weights and external supports are not taken into account. The objects are considered fixed and not affected by the hand while contacts occur.
4. GQMs are computed for up to 100 randomly selected successful grasps per object in order to reduce computational costs. In particular, the 10 GQMs implemented in OpenHand (Q_{A1}, Q_{A2}, Q_{A3}, Q_{B1}, Q_{B2}, Q_{B3}, Q_{C1}, Q_{C2}, Q_{C3}, and Q_{C4}) (León *et al.*, 2014; Rubert *et al.*, 2017) were used.

In order to analyse the grasps generated, some postprocessing was performed in Matlab®. The hand DAs performing grasping postures for each object with the best value for each of the 10 GQMs were identified. The grasps of the hands performing better according to these GQMs were analysed.

2.4. Grasp simulation: anthropomorphic grasp approach

2.4.1. *Generation of GHs*

For the new methodology proposed, the OpenRAVE Grasping Module was extended by the authors with python scripting. The new extension allows the generation of a set of GHs with greater control than that of brute force. These GHs are generated in such a manner that both the relative orientation and relative position of the hand/object in the approaching resemble the natural ones of the human hand. Likewise, the closure of the fingers (step 2 above) varies depending on the GT expected in the human case: all fingers close for CG, but only the thumb and index fingers are considered for PP. The grasps are evaluated with the force-closure condition (as in step 3 above).

For the grasp simulation, a set of different GHs has been generated for each object. The GHs are based on the relative position of the object and the palm (common for all hand DAs). In addition to those defined in Section 2.3, the following new parameters are needed for this approach (see Figs 4 and 5):

1. N_α: Number of approach rays distributed inside the cone with angle α.
2. P: Approach reference point in the hand.
3. $\boldsymbol{n}$: Approach direction vector in the hand.
4. θ_i: Initial roll angle with respect to vector $\boldsymbol{n}$.
5. θ_f: Final roll angle with respect to vector $\boldsymbol{n}$.
6. N_θ: Number of rolls uniformly distributed between θ_i and θ_f.

For each object, only one "target point" is considered in order to generate the approach rays. The selection of this point is made manually based on human experience about how the objects are usually grasped with the intended GT. For some of the objects with geometric symmetry, more than one possible point could be selected, so one of them was arbitrarily chosen. In Fig. 4,

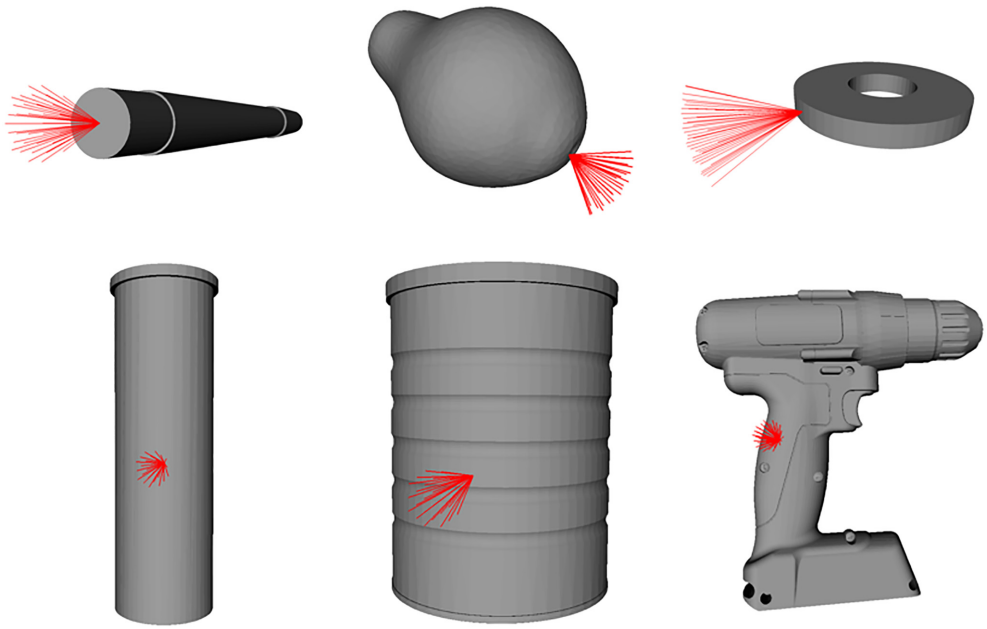

Figure 4: Approach rays considered for each object.

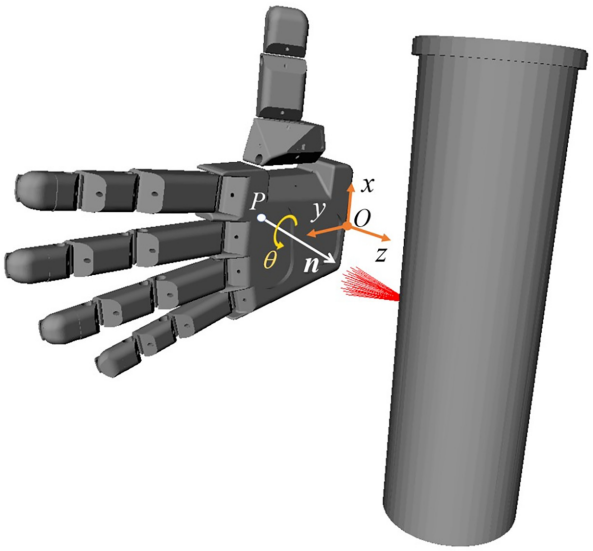

Figure 5: Approach parameters and local coordinate system of the palm.

the approach rays for each object are shown represented as red lines. These sets of rays are defined by two parameters: α and N_α.

In order to define the relative position between the object and the palm, a reference point P and a unit vector $\boldsymbol{n}$ (with origin in the point P) are established in the hand (see Fig. 5). For each ray in the object, the hand approaches toward the object aligning $\boldsymbol{n}$ and the ray. The point P is the same for all the approaches. It is located close to the midpoint between the MCP joints of the index and the middle finger, and its coordinates, defined in the local coordinate system of the palm, are $x = 10$ mm, $y = 70$ mm, $z = 0$ mm. The vector $\boldsymbol{n}$ is slightly different depending on the object to be grasped, and has been chosen to imitate the natural approach of the human hand. A previous representation of the grasp with the baseline of the IMMA hand and each object has been performed in SolidWorks to determine this vector $\boldsymbol{n}$. Moreover, for the CG, the palm approaches toward the object till the contact is reached ($\delta = 0$), but for the PP the fingers of the hand close while the palm remains at a certain standoff distance, imitating the natural human grasp. Table 2 shows all the parameter values selected for generating the GHs. These parameters have been chosen in order to cover a wide range of natural hand–object approaches. The last column shows the total number of GHs tested per object ($N_{GH} = N_\alpha \cdot N_\delta \cdot N_\theta$, where N_δ is the number of standoff distances considered, three for PP and one for CG).

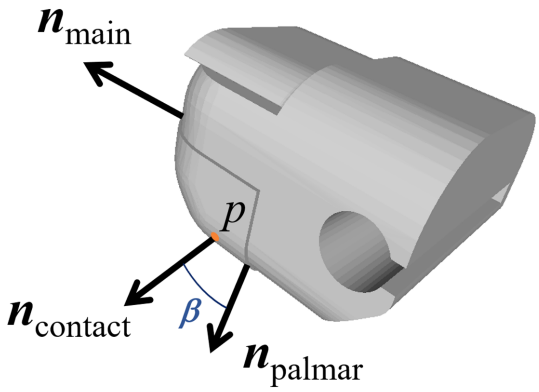

Figure 6: Thumb distal phalanx showing the orientation of the main axis of the thumb, the palmar normal of the finger phalanges, and the normal contact vector.

2.4.2. *Evaluation of anthropomorphic grasp correctness*

For this anthropomorphic grasp approach, we propose to evaluate the grasping postures following the anthropomorphic criteria considered in the AHAP (GT correctness; Llop-Harillo *et al.*, 2019). For each final grasping posture, the developed OpenRAVE extension script is able to automatically evaluate whether the conditions are met or not for an anthropomorphic PP or CG. The grasp correctness criteria are established as follows for each GT:

1. PP: The GT is considered correct if the object contacts with the palmar sides of the distal phalange of the thumb and the distal phalange of only one long finger, without any contact of the object with the palm.
2. CG: The GT is considered correct if the angle between the main axis of the thumb and the main axis of the object's grip area is greater than 60° and there is contact between the object and the palmar sides of the thumb, two phalanges of at least three long fingers and the palm.

To check these conditions, a contact in a point p is considered to happen in the palmar side of a phalanx if the angle β between the normal at that point and the palmar normal vector in this phalanx ($\boldsymbol{n}_{contact}$ and $\boldsymbol{n}_{palmar}$ in Fig. 6) is less than 75°. The thumb main axis direction is defined by a vector $\boldsymbol{n}_{main}$ shown in Fig. 6. For the three CG objects, the main axis of the object's grip area is vertical in Fig. 4.

The GT correctness defined here for the CG is slightly different to that considered in the experimental AHAP (Llop-Harillo *et al.*, 2019), requiring the contact of only two phalanges of the long fingers, instead of three. This slight relaxation of the criterion tries to account for the limitations imposed by the rigid body simulation used in the contact model. If this relaxation is not included, some apparently correct grasps, as the one shown

Table 2: Parameters: selected to generate GHs.

Object	$\boldsymbol{n}$[a]	α (rad)	N_α	δ (mm)	$[\theta_i, \theta_f]$	N_θ	N_{GH}
Small marker	(0, 0, 1)	0.45	38	{45, 50, 55}	[−35°, 35°]	9	1026
Plastic pear	(0.41, 0, 0.91)	0.8	24	{15, 20, 25}	[−35°, 35°]	9	648
Washer	(0, 0, 1)	0.45	38	{45, 50, 55}	[−35°, 35°]	9	1026
Chips can	(0.41, 0, 0.91)	0.2	28	{0}	[−20°, −50°]	15	420
Coffee can	(0.41, 0, 0.91)	0.2	28	{0}	[−20°, −50°]	15	420
Power drill	(0.41, 0, 0.91)	0.5	48	{0}	[−15°, 25°]	15	720

[a] $\boldsymbol{n}$ is defined in the local coordinate system of the palm.

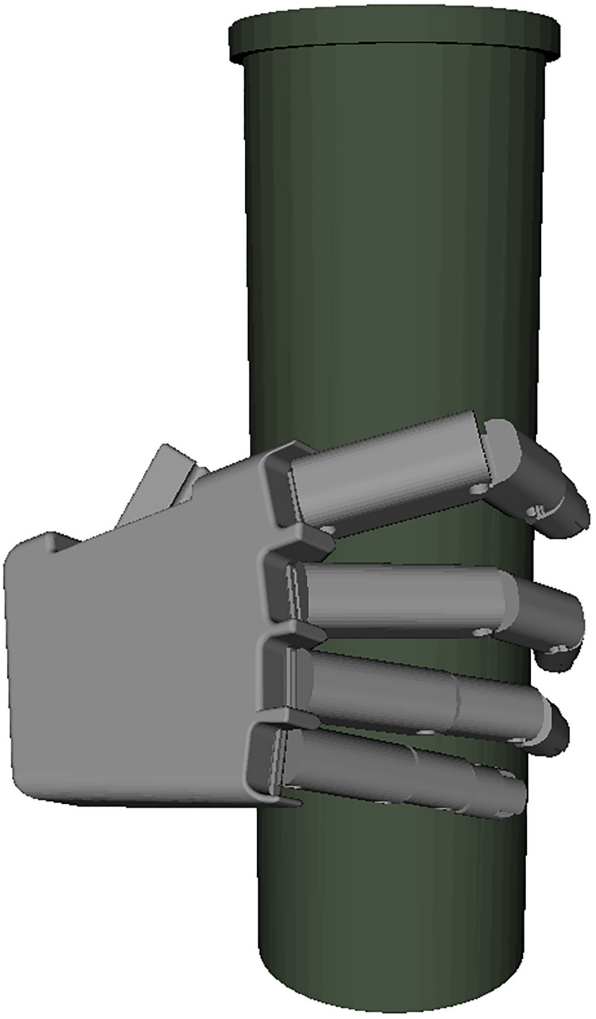

Figure 7: Cylindrical grip that seems anthropomorphic and accomplishes the relaxed correctness criterion but not that of the experimental AHAP.

in Fig. 7, are rejected due to some missing contacts with very small separation between the phalange and the object.

2.4.3. *Simulated grasping ability score*

In order to compare the human-like grasping and the stability of the grasps performed with the different hand DAs, a new index is proposed, adapted from the grasping ability score (GAS) defined in the AHAP (Llop-Harillo *et al.*, 2019). Equation (1) shows the proposed index, named Simulated Grasping Ability Score (S_{GAS}), for each object:

$$S_{GAS_i} = \frac{1}{N_{GH_i}} \left[C_i + 0.5 \cdot NC_i \right], \tag{1}$$

where i refers to the object ($i = 1, \ldots 6$); N_{GHi} is the total number of GHs tested for object i (defined in Section 2.4.1); and C_i and NC_i are, respectively, the number of correct grasps and not correct grasps, according to the GT correctness criteria (Section 2.4.2), on object i, among those satisfying the force-closure condition. The factor 0.5 in equation (1) weights with half-score the force-closure grasps that are not anthropomorphic according to the GT correctness criteria, while the grasps accomplishing both force-closure and GT correctness score 1 point, similarly to the GAS. The S_{GAS} defined in this way ranges between 0 and 1.

In this study, the index has been obtained for the six different objects selected. Moreover, an index per GT has also been obtained [equation (2) with $n = 3$], averaging the index of the different objects considered for each GT, and a total index has been obtained averaging the index of all the objects [equation (2) with $n = 6$].

$$S_{GAS} = \frac{1}{n} \sum_{i=1}^{n} S_{GAS_i} \tag{2}$$

3. Results

3.1. Brute-force approach

Table 3 shows, for each object, the IMMA hand DA that performed the best grasp according to each of the GQMs included in OpenHand. The washer does not appear in this table because none of the grasps performed with this object was a successful grasp according to the force-closure condition. The DA with thumb CMC 15° and MCP 90° performed most of those best grasps (7/50). It was followed by the DA with thumb CMC 30° and MCP 15° (4/50) that obtained the best grasps according to the GQM only for one object (chips can) and the DA with thumb CMC 0° and MCP 60° (4/50) that obtained the best results for four of the objects (plastic pear, chips can, coffee can, and power drill). The rest of DAs appear less than three times. Figure 8 shows the grasps with the best GQM performed by the best hand design according to this approach (CMC 15° and MCP 90°). It can be seen that none of the grasps resemble those shown in Fig. 2 and most of the grasp postures are weird from a human perspective.

3.2. Anthropomorphic grasp approach

Figure 9a shows the results of total S_{GAS} versus MCP angle for each CMC angle. Among the hand DAs analysed changing CMC and MCP thumb angles, the best total S_{GAS} (47%) was obtained for that with CMC 30° and MCP 75°. Figure 9b shows a 2D contour plot representation of the results obtained for total S_{GAS} by spline interpolation (grid spacing 1°) from the computed DAs. The optimal design according to the total S_{GAS} is close to CMC 20°–30° and MCP 65°–75°. The baseline obtained a total S_{GAS} of 24%.

Figure 10 shows the mean and standard deviation across hand DAs of the number of grasps that accomplish the force-closure condition (FC) and the number of grasps that accomplish both the force-closure condition and the GT correctness (C), for each object analysed along with the number of tested GHs (N_{GH}). It is worth noting that NC in equation (1) can be obtained as the difference between FC and C. For the PP objects (small marker, plastic pear, and washer), the difference between FC and C is small. However, for the CG objects (chips can, coffee can, and power drill), this difference is higher because the number of correct grasps is low. Notwithstanding, the force-closure condition is obtained in a greater fraction of the tested GHs for CG.

Figure 11 shows, for the best hand DA, one of the grasps accomplishing GT correctness for each object.

4. Discussion

This study is focused on assessing and comparing prosthetic hand designs according to the anthropomorphism of the simulated grasps performed. According to our results, the brute-force approach and the evaluation with GQM have evident limitations for evaluating grasping anthropomorphism of artificial hands for the main GTs. Figure 8 shows that some of the best grasps

Table 3: Hand: designs (CMC angle – MPC angle) that scored highest for each of the 10 GQMs for the different objects.

	Q_{A1}	Q_{A2}	Q_{A3}	Q_{B1}	Q_{B2}	Q_{B3}	Q_{C1}	Q_{C2}	Q_{D1}	Q_{D2}
Small marker	30°–90°	15°–90°	30°–90°	30°–75°	15°–90°	15°–90°	30°–75°	45°–90°	15°–90°	15°–90°
Plastic pear	30°–30°	30°–45°	30°–30°	15°–75°	30°–75°	0°–60°	45°–45°	45°–30°	30°–60°	15°–0°
Chips can	30°–15°	30°–15°	30°–45°	45°–45°	30°–15°	15°–90°	0°–60°	30°–15°	30°–60°	30°–0°
Coffee can	0°–90°	30°–45°	0°–90°	45°–45°	45°–15°	0°–60°	0°–30°	45°–15°	30°–30°	30°–0°
Power drill	45°–0°	45°–0°	0°–45°	0°–45°	45°–0°	0°–60°	15°–15°	45°–90°	15°–90°	15°–0°

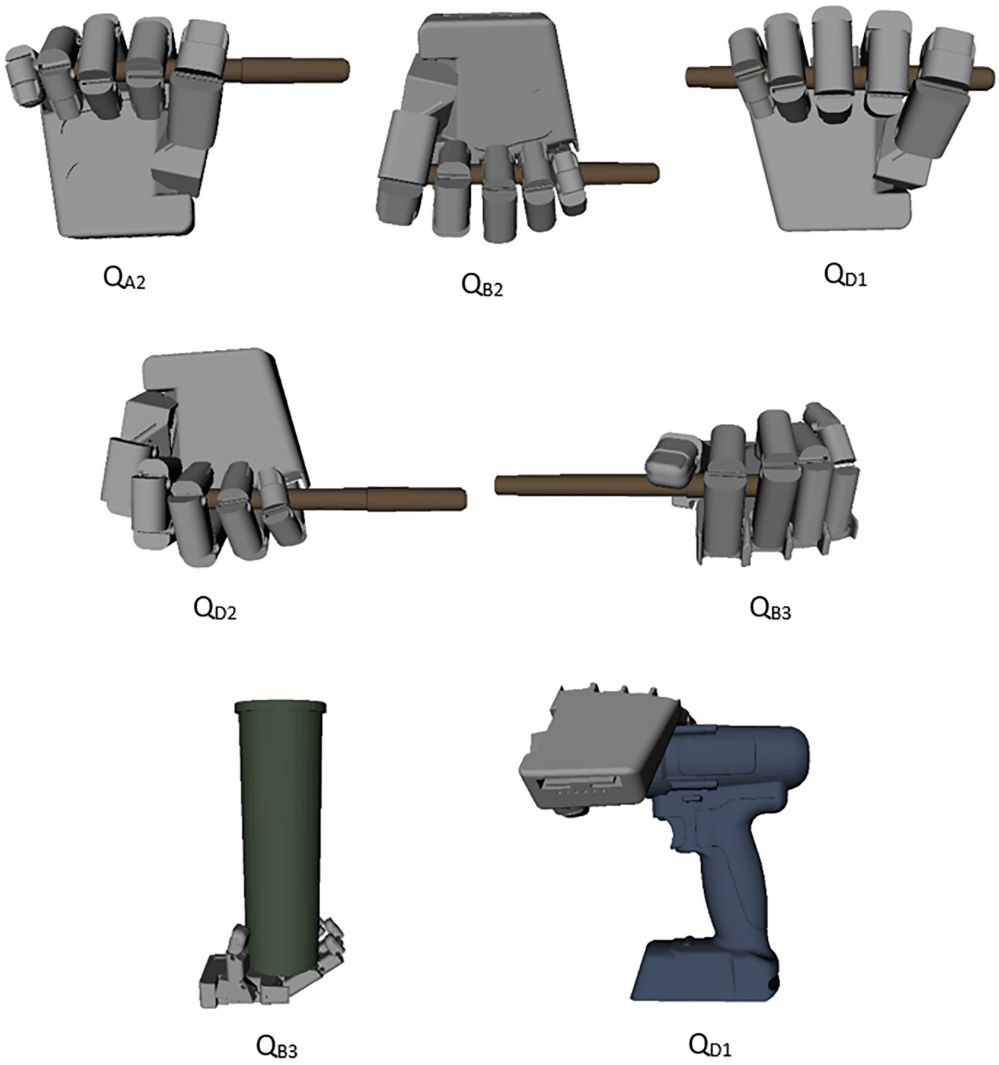

Figure 8: Grasps with the best GQMs performed by the IMMA hand DA with thumb CMC 15° and MCP 90°.

selected with this approach do not fulfill the criteria of anthropomorphism defined in the literature (Sollerman & Ejeskär, 1995; Vergara *et al.*, 2014; Llop-Harillo *et al.*, 2019) for the expected GTs (PP and CG). Moreover, the majority of the grasps obtained with this approach are not realistic for the expected use of the objects by a human in ADL. The simulation benchmark proposed in this study allows undertaking the comparison of hand DAs based on anthropomorphic criteria apart from being more efficient in terms of computation time. The final grasps obtained with this approach are more meaningful in terms of anthropomorphism and ADL (see Fig. 11). The fact that the position of the target point for the GHs is unique in the procedure is not a relevant limitation, because in prosthetic hands the users select the approaching point for the grasp. The different GHs generated around this target point evaluate the robustness of each DA for achieving the correct grasp under slight variations in orientation or position.

A noteworthy advantage of the simulation benchmark proposed is the reduced time required to compare different hand DAs against the experimental approach. In this study, 28 different DAs of the thumb CMC and MCP joint orientations have been analysed easily. An experimental comparison for such a big number of alternatives would be unaffordable in a reasonable time.

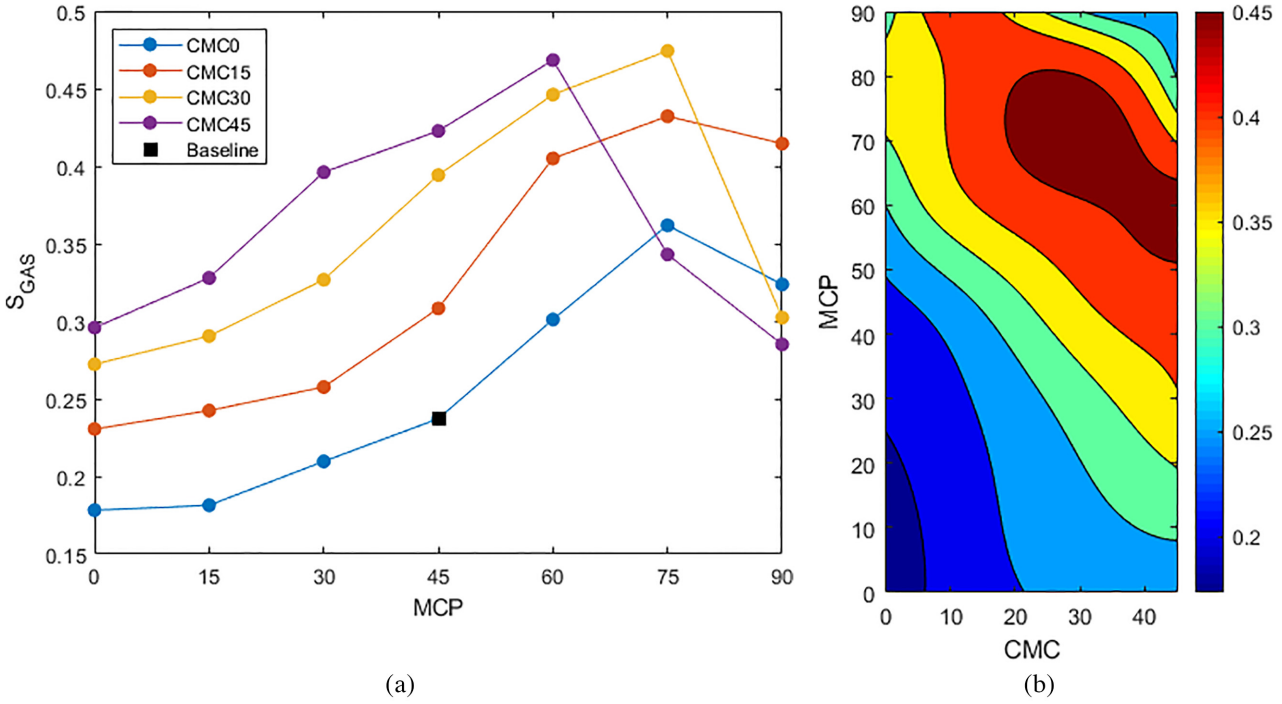

Figure 9: (a) Total S_{GAS} as a function of MCP angle for each CMC angle; (b) total S_{GAS} as a function of CMC and MCP angles, obtained by spline interpolation (grid spacing 1°) from the computed DAs.

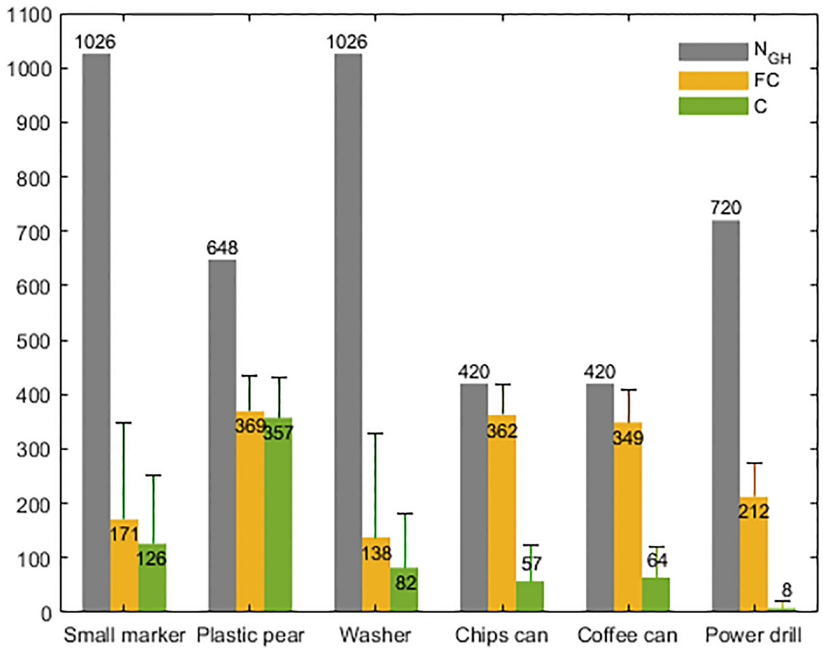

Figure 10: Mean and standard deviation of force-closure grasps (FC) and correct grasps (C) across hand DAs for each object.

Among the DAs tested here for the IMMA hand, the best result on S_{GAS} was obtained using CMC 30° and MCP 75°. Figure 9a shows that DAs with CMC 45° and MCP between 45° and 60°, those with CMC 30° and MCP between 60° and 75°, and those with CMC 15° and MCP between 75° and 90° obtained similar values on total S_{GAS}. It is worth noting that for these DAs the sum of CMC and MCP angles ranges between 90° and 105°. These orientations allow a good opposition between the thumb and index fingers needed to perform PP as well as a good orientation of the thumb with respect to the main axis of the object grip area, needed to perform correctly CG. Other thumb joint orientations with a lower or higher sum of angles are not so suitable to perform these anthropomorphic grasps. Figure 9b shows this trend because the highest scores are found in a fringe where CMC and MCP orientation angles sum around 100°. A deeper analysis of the results, not shown here for brevity but available in Table A1

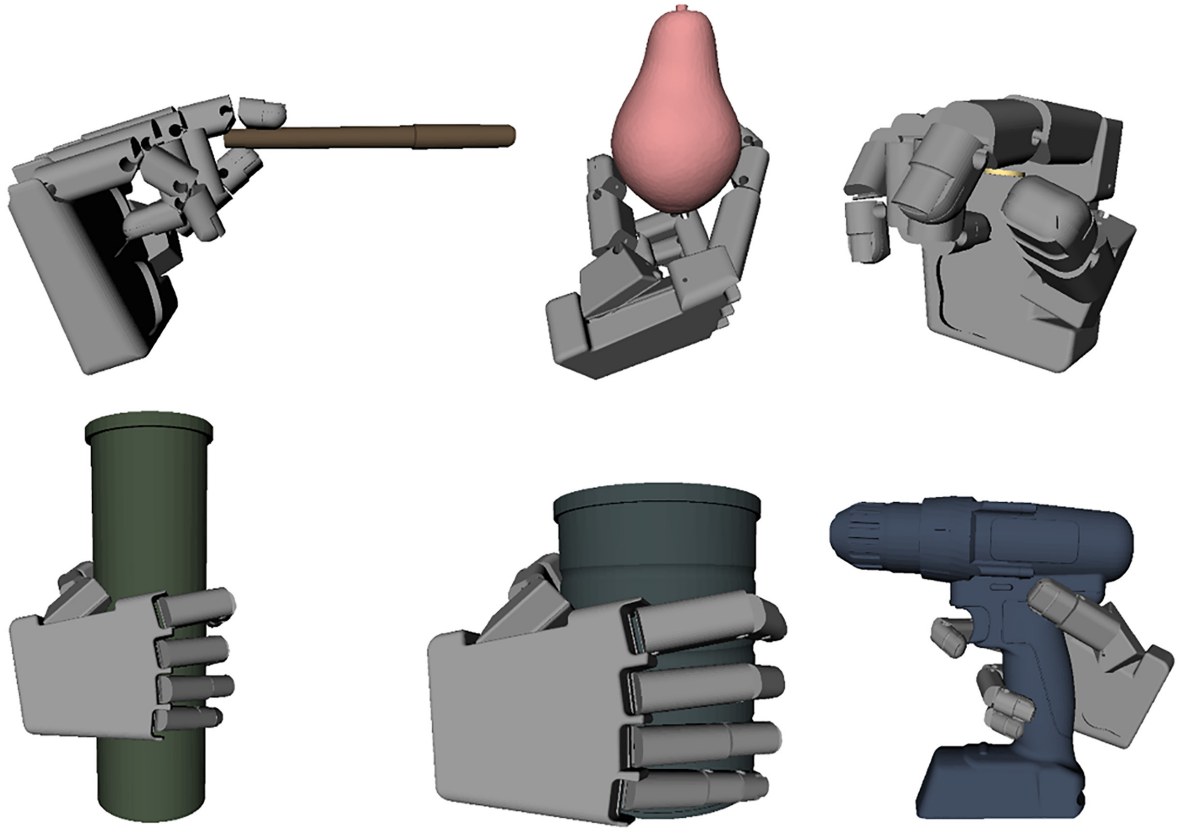

Figure 11: Correct grasps performed with the IMMA hand DA with thumb CMC 30° and MCP 75°.

in the appendix, indicates that for some hand DAs, located in the bottom-left and top-right corners of this figure, the value of S_{GAS} is even null for the PP with the small marker and very low for the washer, because for those DAs the opposition of the thumb to the index finger does not allow to reach the force-closure condition.

Nevertheless, the limitations of the simulation framework should be considered in its predictive performance. The method used in OpenRAVE to obtain the final grasping posture could explain the problem to reach correct grasps for CG in the simulation, especially for objects with a complex shape (such as the power drill). This is because the motion of a finger stops if the distal segment contacts first with the object, making impossible in such cases the contact with the proximal phalanges. Additionally, due to the method used in OpenRAVE to simulate the closing motion of the fingers, which considers the thumb as a unique kinematic chain, the CMC joint of the thumb closes completely before the MCP joint begins to close. This limitation has special relevance on obtaining the right orientation angles of the thumb joints that allow the opposition with the index finger, necessary for force-closure and GT correctness in PP. To improve thumb opposition, it is useful to control independently these two DoFs of the thumb (CMC and MCP), as in the actual prototype (baseline) of the IMMA hand (Llop-Harillo *et al.*, 2020). However, due to the limitations explained above, this independent motion is not possible in OpenRAVE.

Notwithstanding the limitations of this simulation analysis, the anthropomorphic approach proposed in this study offers a good benchmark to evaluate anthropomorphic grasps in order to select optimal hand DAs. This benchmark is based only on the two most frequent GTs, despite the experimental AHAP being composed of eight GTs. In the near future, we plan to include all these GTs in the simulated benchmark in order to make the assessment of hand DAs more representative of ADL, and to validate it by means of the experimental AHAP.

5. Conclusions

In this study, two different simulation approaches focused on assessing grasping in prosthetic hand designs have been compared with the aim of obtaining a useful metric to measure their anthropomorphism and functionality during ADL.

The combination of the brute-force approach for generating GHs and GQM for the evaluation of the final grasping posture, used in previous works in the literature, resulted in neither anthropomorphic nor realistic grasps for the expected use of the objects by a human.

A new simulation benchmark has been proposed that follows an anthropomorphic approach for defining the GHs and for assessing hand designs. The main improvements provided by the new method are as follows:

1. It reduces the computational cost, taking profit of the human experience for limiting the number of GHs, avoiding redundancies due to symmetry, and preventing nonanthropomorphic grasps.
2. Its principles are adapted from the experimental benchmark AHAP and it considers GT correctness criteria for assessing the anthropomorphism of the final grasps.
3. It resulted in more anthropomorphic and realistic grasps than the brute-force approach.

4. The metric associated with the benchmark allows the comparison of different hand DAs in order to obtain optimal solutions.

In a comparison of 28 different DAs of the IMMA hand changing the orientation of the CMC and MCP joints of the thumb with respect to the baseline design, the new benchmark has allowed us to define preferable orientations for these joints in order to improve significantly the number of successful and anthropomorphically correct grasps for PP and CG, the most frequent GTs. In the near future, this proposal will be completed including all the main GTs used in ADL and considered in the AHAP, and it will be experimentally validated.

Acknowledgments

This work was supported by the Spanish Ministry of Economy and Competitiveness and ESF (grant number BES-2015–076005); the Spanish Ministry of Economy and Competitiveness, AEI, and ERDF (grant numbers DPI2014-60635-R and DPI2017-89910-R); Universitat Jaume I, Spain (grant number UJI-B2017-70); and Generalitat Valenciana (Spain) (grant number GV/2018/125). This publication is also part of the R + D project PID2020-118021RB-100, funded by MICIN/AEI/10.13039/501100011033.

We also acknowledge Carlos Rubert for his contribution in the integration of the hands in the simulation framework and in the simulations performed with OpenHand.

Conflict of interest statement

None declared.

References

Belter, J. T., Segil, J. L., Dollar, A. M., & Weir, R. F. (2013). Mechanical design and performance specifications of anthropomorphic prosthetic hands: A review. *The Journal of Rehabilitation Research and Development*, *50*, 599–617.

Calli, B., Walsman, A., Singh, A., Srinivasa, S., Abbeel, P., & Dollar, A. M. (2015). Benchmarking in manipulation research: Using the Yale-CMU-Berkeley object and model set. *IEEE Robotics & Automation Magazine*, *22*, 36–52.

Ciocarlie, M., Miller, A., & Allen, P. (2005). Grasp analysis using deformable fingers. In *2005 IEEE/RSJ International Conference on Intelligent Robots and Systems*. IEEE, (pp.4122–4128).

Diankov, R. (2010). *Automated construction of robotic manipulation programs, Architecture Ph.D.* (pp. 1–263).

Falco, J., Van Wyk, K., Liu, S., & Carpin, S. (2015). Grasping the performance: Facilitating replicable performance measures via benchmarking and standardized methodologies. *IEEE Robotics & Automation Magazine*, *22*, 125–136.

Feix, T., Romero, J., Ek, C. H., Schmiedmayer, H. B., & Kragic, D. (2013). A metric for comparing the anthropomorphic motion capability of artificial hands. *IEEE Transactions on Robotics*, *29*, 82–93.

Huamán Quispe, A., Ben Amor, H., & Christensen, H. I. (2018). A taxonomy of benchmark tasks for robot manipulation. In *Springer Proceedings in Advanced Robotics*. (pp. 405–421).

Jang, C. H., Yang, H. S., Yang, H. E., Lee, S. Y., Kwon, J. W., Yun, B. D., Choi, J. Y., Kim, S. N., & Jeong, H. W. (2011). A survey on activities of daily living and occupations of upper extremity amputees. *Annals of Rehabilitation Medicine*, *35*, 907.

León, B., Ulbrich, S., Diankov, R., Puche, G., Przybylski, M., Morales, A., Asfour, T., Moisio, S., Bohg, J., Kuffner, J., & Dillmann, R. (2010). OpenGRASP: A toolkit for robot grasping simulation. In *Lecture Notes in Computer Science (Including Subseries Lecture Notes in Artificial Intelligence and Lecture Notes in Bioinformatics)*. (pp. 109–120).

León, B., Sancho-Bru, J. L., Jarque-Bou, N. J., Morales, A., & Roa, M. A. (2012). Evaluation of human prehension using grasp quality measures. *International Journal of Advanced Robotic Systems*, *9 (4)*.

León, B., Rubert, C., Sancho-Bru, J., & Morales, A. (2013). Evaluation of prosthetic hands prehension using grasp quality measures. In *2013 IEEE/RSJ International Conference on Intelligent Robots and Systems*. IEEE, (pp. 3501–3506).

León, B., Morales, A., & Sancho-Bru, J. (2014). *From robot to human grasping simulation, cognitive systems monographs, cognitive systems monographs*. Springer International Publishing.

Levine, S., Pastor, P., Krizhevsky, A., Ibarz, J., & Quillen, D. (2018). Learning hand-eye coordination for robotic grasping with deep learning and large-scale data collection. *The International Journal of Robotics Research*, *37*, 421–436.

Liarokapis, M. V., Artemiadis, P. K., & Kyriakopoulos, K. J. (2013). Quantifying anthropomorphism of robot hands. In *Proceedings of the IEEE International Conference on Robotics and Automation*. IEEE, (pp. 2041–2046).

Lin, Y., & Sun, Y. (2015). Robot grasp planning based on demonstrated grasp strategies. *The International Journal of Robotics Research*, *34*, 26–42.

Llop-Harillo, I., & Pérez-González, A. (2017a). System for the experimental evaluation of anthropomorphic hands. Application to a new 3D-printed prosthetic hand prototype. *International Biomechanics*, *4*, 50–59.

Llop-Harillo, I., & Pérez-González, A. (2017b). IMMA hand (Devalhand project) [WWW Document]. URL https://sites.google.com/a/uji.es/devalhand/imma-hand (accessed 11.18.19).

Llop-Harillo, I., Pérez-González, A., Starke, J., & Asfour, T. (2019). The Anthropomorphic Hand Assessment Protocol (AHAP). *Robotics and Autonomous Systems*, *121*, 103259.

Llop-Harillo, I., Pérez-González, A., & Andrés-Esperanza, J. (2020). Grasping ability and motion synergies in affordable tendon-driven prosthetic hands controlled by able-bodied subjects. *Frontiers in Neurorobotics*, *14*.

Miller, A. T., & Allen, P. K. (2004). Graspit: A versatile simulator for robotic grasping. *IEEE Robotics Automation Magazine*, *11*, 110.

Moisio, S., Leon, B., Korkealaakso, P., & Morales, A. (2012). Simulation of tactile sensors using soft contacts for robot grasping applications. In *2012 IEEE International Conference on Robotics and Automation*. IEEE, (pp. 5037–5043).

Morales, A., Chinellato, E., Fagg, A. H., & Del Pobil, A. P. (2004). Using experience for assessing grasp reliability. *International Journal of Humanoid Robotics*, *1*, 671–691.

Nguyen, V. (1986). Constructing force-closure grasps. In *IEEE International Conference on Robotics and Automation*. (pp. 1368–1373).

Pérez-González, A., & Llop-Harillo, I. (2019). *3D models of the objects selected (from YCB set) for the different grasp types in the Anthropomorphic Hand Assessment Protocol (AHAP)*. Available at: https://doi.org/10.5281/zenodo.3560735.

Pinto, L., & Gupta, A. (2016). Supersizing self-supervision: Learning to grasp from 50K tries and 700 robot hours. In *2016 IEEE International Conference on Robotics and Automation (ICRA)*. IEEE, (pp. 3406–3413).

Roa, M. A., & Suárez, R. (2014). Grasp quality measures: Review and performance. *Autonomous Robots*, *38*, 65–88.

Rubert, C., & Morales, A. (2016). Comparison between grasp quality metrics and the anthropomorphism index for the evaluation of artificial hands. In *2016 6th IEEE International Conference on Biomedical Robotics and Biomechatronics (BioRob)*. IEEE, (pp. 1352–1357).

Rubert, C., León, B., Morales, A., & Sancho-Bru, J. (2017). Characterisation of grasp quality metrics. *Journal of Intelligent & Robotic Systems*, *89*, 319–342.

Sahbani, A., El-Khoury, S., & Bidaud, P. (2012). An overview of 3D object grasp synthesis algorithms. *Robotics and Autonomous Systems*, *60*, 326–336.

Sollerman, C., & Ejeskär, A. (1995). Sollerman hand function test: A standardised method and its use in tetraplegic patients. *Scandinavian Journal of Plastic and Reconstructive Surgery and Hand Surgery*, *29*, 167–176.

Vergara, M., Sancho-Bru, J. L., Gracia-Ibáñez, V., & Pérez-González, A. (2014). An introductory study of common grasps used by adults during performance of activities of daily living. *Journal of Hand Therapy: Official Journal of the American Society of Hand Therapists*, *27*, 1–28.

Appendix 1

Table A1: Results of the new simulation benchmark for the different DAs of the IMMA hand analysed.

IMMA DAs		Small marker			Plastic pear			Washer			Chips can			Coffee can			Power drill			PP	CG	Total
CMC (°)	MCP (°)	FC (%)	C (%)	S_{GAS} (%)	FC (%)	C (%)	S_{GAS} (%)	FC (%)	C (%)	S_{GAS} (%)	FC (%)	C (%)	S_{GAS} (%)	FC (%)	C (%)	S_{GAS} (%)	FC (%)	C (%)	S_{GAS} (%)	S_{GAS} (%)	S_{GAS} (%)	S_{GAS} (%)
0	0	0.0	0.0	0.0	31.8	30.2	31.0	0.4	0.0	0.2	66.2	0.0	33.1	61.7	5.2	33.5	18.3	0.0	9.2	10.4	25.2	**17.8**
0	15	0.0	0.0	0.0	36.7	34.4	35.6	0.4	0.0	0.2	63.3	1.0	32.1	56.7	9.5	33.1	15.7	0.0	7.8	11.9	24.4	**18.1**
0	30	0.0	0.0	0.0	45.8	45.4	45.6	0.4	0.0	0.2	62.9	4.0	33.5	57.9	18.3	38.1	16.9	0.0	8.5	15.3	26.7	**21.0**
0[a]	45	2.8	2.5	2.7	54.2	54.2	54.2	0.4	0.0	0.2	63.1	10.2	36.7	58.8	23.6	41.2	14.9	0.0	7.4	19.0	28.4	**23.7**
0	60	22.1	20.6	21.3	55.4	55.4	55.4	3.7	2.9	3.3	64.0	26.2	45.1	63.6	29.3	46.4	18.2	0.0	9.1	26.7	33.5	**30.1**
0	75	34.8	27.9	31.3	53.4	53.4	53.4	20.7	18.7	19.7	71.9	39.5	55.7	66.7	28.3	47.5	18.2	0.8	9.5	34.8	37.6	**36.2**
0	90	29.9	23.7	26.8	48.3	45.7	47.0	27.4	24.9	26.1	68.1	19.8	43.9	62.4	17.4	39.9	17.9	3.2	10.6	33.3	31.5	**32.4**
15	0	0.0	0.0	0.0	41.7	39.8	40.7	0.4	0.0	0.2	86.2	0.0	43.1	81.0	0.0	40.5	27.6	0.0	13.8	13.6	32.5	**23.1**
15	15	0.0	0.0	0.0	48.6	48.1	48.4	0.4	0.0	0.2	84.8	0.0	42.4	79.8	1.7	40.7	27.6	0.0	13.8	16.2	32.3	**24.2**
15	30	0.8	0.8	0.8	57.1	57.1	57.1	0.4	0.0	0.2	81.4	0.0	40.7	78.3	4.5	41.4	28.6	0.1	14.4	19.4	32.2	**25.8**
15	45	17.4	15.9	16.7	62.5	62.5	62.5	2.8	2.6	2.7	81.9	1.7	41.8	79.3	13.3	46.3	30.0	0.0	15.0	27.3	34.4	**30.8**
15	60	37.0	28.0	32.5	62.5	62.5	62.5	20.4	18.3	19.3	85.2	26.4	55.8	85.0	31.7	58.3	28.1	1.0	14.5	38.1	42.9	**40.5**
15	75	32.7	25.1	28.9	57.4	57.4	57.4	28.4	25.1	26.8	88.1	44.5	66.3	88.6	40.7	64.6	26.1	4.4	15.3	37.7	48.7	**43.2**
15	90	41.7	25.0	33.3	54.6	49.7	52.2	59.6	18.9	39.2	83.8	24.5	54.2	84.0	28.3	56.2	25.3	2.1	13.7	41.6	41.3	**41.5**
30	0	0.0	0.0	0.0	51.7	50.9	51.3	0.4	0.0	0.2	96.7	0.0	48.3	93.6	0.0	46.8	33.5	0.0	16.7	17.2	37.3	**27.2**
30	15	0.1	0.0	0.0	61.6	61.6	61.6	0.4	0.0	0.2	96.2	0.0	48.1	94.8	0.0	47.4	34.0	0.0	17.0	20.6	37.5	**29.1**
30	30	13.3	11.9	12.6	67.4	67.4	67.4	3.2	2.5	2.9	95.5	0.0	47.7	94.0	0.2	47.1	36.7	0.0	18.3	27.6	37.7	**32.7**
30	45	37.1	27.3	32.2	68.7	68.7	68.7	20.1	17.1	18.6	95.5	5.0	50.2	92.1	4.3	48.2	36.5	0.8	18.7	39.8	39.0	**39.4**
30	60	34.6	26.3	30.5	64.8	64.8	64.8	27.7	23.5	25.6	97.9	30.2	64.0	96.0	27.6	61.8	37.4	4.7	21.0	40.3	49.0	**44.6**
30	75	41.7	23.9	32.8	59.6	59.6	59.6	57.1	17.2	37.1	96.7	44.3	70.5	95.0	35.2	65.1	35.8	3.2	19.5	43.2	51.7	**47.4**
30	90	0.0	0.0	0.0	56.2	46.5	51.3	0.4	0.0	0.2	93.8	17.4	55.6	91.0	26.4	58.7	30.6	0.7	15.6	17.2	43.3	**30.2**
45	0	0.0	0.0	0.0	61.7	61.7	61.7	0.4	0.0	0.2	99.3	0.0	49.6	94.5	0.0	47.3	37.4	0.0	18.7	20.6	38.5	**29.6**
45	15	7.8	7.2	7.5	69.9	69.9	69.9	2.8	1.4	2.1	98.8	0.0	49.4	93.8	0.0	46.9	41.9	0.0	21.0	26.5	39.1	**32.8**
45	30	36.5	27.5	32.0	71.8	71.8	71.8	16.9	13.5	15.2	99.8	1.0	50.4	94.8	0.0	47.4	41.5	0.6	21.0	39.6	39.6	**39.6**
45	45	34.4	26.6	30.5	69.0	69.0	69.0	26.0	21.9	24.0	99.5	12.4	56.0	96.7	4.8	50.7	42.1	5.0	23.5	41.2	43.4	**42.3**
45	60	41.3	24.0	32.7	63.9	63.9	63.9	54.6	15.5	35.0	99.8	34.5	67.1	95.7	23.8	59.8	41.0	4.2	22.6	43.9	49.8	**46.8**
45	75	0.0	0.0	0.0	59.7	57.1	58.4	0.4	0.0	0.2	98.3	33.1	65.7	95.2	32.1	63.7	34.9	0.8	17.8	19.5	49.1	**34.3**
45	90	0.0	0.0	0.0	60.3	35.6	48.0	0.4	0.0	0.2	97.4	6.0	51.7	93.1	20.0	56.5	29.3	0.0	14.7	16.1	41.0	**28.5**

[a] Baseline.